CANDU FUEL COMPRESSION TESTS AT ELEVATED TEMPERATURES

E. KØHN, J.K. CHAN, V.J. LANGMAN, G.I. HADALLER* and R.A. FORTMAN*

Ontario Hydro, 700 University Ave.,Toronto, Ontario, M5G 1X6
*Stern Laboratories, Hamilton, Ontario, L8H 3L3

ABSTRACT

An inlet header large break loss of coolant accident (LOCA) in CANDU reactors with fuelling against flow can cause the fuel to shift in the channels with a consequent reactivity insertion. This results in an increased fuel power transient, and a potential increase in the analyzed consequences for such events. As the reactors age and the channel axial gaps increase, the magnitude of the predicted power transient increases. A design solution to reduce the power transient is to limit the amount of fuel movement by reducing the channel axial gap. This solution was implemented into Ontario Hydro's Bruce B and Darlington reactors.

A consequence of a reduced channel axial gap is the potential for the fuel column axial expansion to become constrained by the channel end components in large break LOCAs. This experimental program investigated the effects of pellet cracking and elevated sheath temperatures on the ability of the fuel elements, of the 37-element bundle design, to sustain axial loads. The unirradiated fuel elements tested were either in the as-received condition or with the UO_2 fuel pellets cracked in a mechanical process to simulate the effect of irradiation. The load deformation characteristics demonstrated that, for a given amount of axial compression, the loads sustainable by the elements at elevated sheath temperatures were low. As a result, excess axial expansion would be easily accommodated without further challenge to pressure tube integrity.

INTRODUCTION

In March 1993, the positive reactivity issue was assessed in some of Ontario Hydro's reactors with respect to large break LOCAs[1]. The issue was associated with fuel string movement during an inlet header break, which causes an increase in the power transient experienced by the fuel. As the reactors age, the axial pressure tube creep results in an increased axial gap in the channel between the inlet fuel bundle and the inlet shield plug. With increasing channel axial gap, the magnitude of possible relocation increases, which causes a resulting increase in the level of the power transient during the first few seconds in RIH large break LOCAs. A design solution to lower the power transient is to reduce the channel axial gap by the introduction of long fuel bundles, flow straightening inlet shield plugs, and a gap management system. This solution has been implemented into Ontario Hydro's Bruce B and Darlington reactors.

Another reason to minimize the axial gap is to relocate the fuel onto the spacer sleeve to avoid burnish mark fretting on the pressure tube. The burnish mark is a high stress location and it is very desirable to avoid fretting at this position. The result was that the minimum gap that could reasonably be accommodated, considering all the factors, was 32 mm (1.25 inch). However, this led to another concern that during large break LOCAs, the fuel string could, in a limited number of high power channels, expand axially into contact with the ends of the fuel channel. The expanding fuel column, constrained between the fuel latch at the channel outlet and the flow straightening inlet shield plug, exerts an axial load on the channel components.

The channel axial gap needs to be minimized in order to reduce the fuel movement and the potential overpower transient during a LOCA. At the same time it is desirable to reduce fretting at the burnish mark. An axial gap management system simultaneously accomplishes these tasks. This system uses long fuel bundles and flow straightening inlet shield plugs to control the axial gap. The quantification of the axial loads in this program demonstrates that the loads are sufficiently low that channel integrity is assured.

This paper discusses tests performed on single outer fuel elements, both with initially intact and cracked pellets, at uniform temperatures of 300 to 1100 °C. The compression load "stiffness" determined from the cracked fuel elements, in the temperature range 800 to 1000 °C, was found to be approximately 0.5 kN/mm. This is considerably lower than the value of 14 kN/mm used in the recent analysis of high temperature behaviour under conditions of axial restraint[2].

BACKGROUND

Past experimental programs were generally not designed to assist in the investigation of axial compression of CANDU fuel during high temperature transients. Therefore, the information used in the safety analysis of this type of event was developed from low temperature tests which did not take into account the effect of sheath temperatures in reducing the strength and the resulting compliance of the fuel column.

Single element compression tests at room temperature were completed at AECL-CRL[3]. These tests were completed in support of the Darlington N12 program which was investigating the effect of irradiated fuel on the spring constant of the fuel string. In this program, two series of tests were completed. The first series was a compression of the fuel element including endcaps. In the second series, the tests used a direct load applied to the fuel pellet column within the fuel sheath (up to 2 kN). The loading of the fuel elements was applied through a simple lever arm loaded with a series of weights. In order to avoid element deflection at the higher loads, a restraining ring was located at the element centre. The fuel used for these tests was irradiated in Darlington. The elements were loaded up to 2 kN. The load deformation curves indicated that the main contribution at low loads was the element axial stiffness of the fuel sheath. The element stiffness was measured as 2.79 kN/mm. It was noted that at higher loads there was a hysteresis effect due to the combined effect of the sheath and the UO_2 column. At the highest load, the element modulus was estimated as 42 GPa. Note that before measurements were made, the fuel stack was compressed repeatedly to pack pellet pieces together; therefore, high loads were expected in these tests.

When the upper endcaps were removed in order to apply the loads directly to the UO_2 fuel stack, the end pellets were easily removed as fragments about 1 - 5 mm in size.

If the UO_2 fuel column became supporting, then the effective modulus of the element would increase. The value of the modulus is stress dependent as it effectively depends on the compression of the cracks; as they compress, the effective contact surface increases[4], leading to a higher effective modulus. The initial modulus can be expected to be quite low in CANDU fuel because the initial pellet loads are only about 160 N. Thus, considerable elastic compression of the fuel stack would be expected before the modulus becomes high.

The fragment sizes can be estimated from photographs in Reference 4. The variation of fuel cracking with power for CANDU fuel shows that a cross section of a pellet contains many fragments[5] (about 40 distinct pieces in a 50 kW/m element section). Each pellet can be considered an assembly of fragments and cannot be expected to support significant axial loads, unless restrained within the sheath. Thus, the sheath and fuel pellet fragment column becomes the structural assembly. The restraint of the sheath provides the forces to prevent the pellet fragments from falling away at minimal load. The higher the radial restraint by the fuel sheath, the more the UO_2 column could be expected to act as an integral structure. However, at high temperatures, the sheath is weak, and will only provide a small amount of radial constraint to the diametral expansion of the UO_2 column. Thus, a temperature dependent relation which would follow the plastic flow characteristics of the fuel sheath is expected.

EXPERIMENTAL

Single element compression tests were conducted on outer fuel elements, of the 37-element bundle design, compressed between end supports. The elements were axially aligned and constrained concentrically at the ends within an externally heated tube to simulate the fuel temperature and radial clearance of an element within a fuel bundle. Fresh outer fuel elements were cut from production fuel bundles. The outer elements are of most interest since they are predicted to experience more constrained expansion. The end plates were included in some initial tests, but most tests had the end plate and the spigot of the endcap removed to determine the separate effects of the compression of the fuel element, rather than the spigot/endcap effect. The following provides a more complete description of the tests.

A schematic of the test apparatus is shown in Figure 1. It consists of a 0.6 metre long, 3/4 inch schedule 160 stainless steel pipe test section. The measured bore of the pipe is 16.00 mm that yields a nominal clearance of 0.64 mm to the element mid-plane appendages (sheath outside diameter is 13.12 mm). Each end of the test section is equipped with a loading head, one fixed and one traversing. The loading heads serve to maintain concentricity of the element at the endcaps while applying the load to the end plate segment only and provide penetrations for purge gas and thermocouples.

The fixed loading head is mounted to a load cell to measure the applied axial load and has a penetration for five thermocouples leads. Three thermocouples are located along the element and one at each end plate segment. The loading head and the load cell are separated by a zirconia cup which provides a thermal barrier to minimize axial heat loss and prevent damage to the load cell due to high temperatures.

The traversing loading head is mounted to the hydraulic ram and has a bellows installed which allows up to 25 mm of un-restrained axial travel. A zirconia cup is also installed at this end to minimize axial heat loss. The axial travel is measured using a calibrated linear potentiometer which has a resolution of ± 0.10 mm (1σ). The maximum travel is limited to 25 mm by a limit switch that automatically stops the hydraulic ram extension. This limit is adjustable to any amount less than 25 mm as required. The hydraulic fluid circuit is equipped with flow and back pressure control valves which are required to set the rate of deformation, the creep load and the maximum load.

The test section is enclosed with six semicircular and equal length ceramic insulated heaters capable of operating up to 1100°C. These heaters are independently powered to minimize temperature gradients along the length. Three type K thermocouples are mounted on the outside of the test section. These thermocouples monitor the heater temperatures and provide for over-temperature protection of the heaters.

The temperatures are measured by premium grade, 0.5 mm diameter, ungrounded, ANSI type K thermocouples. The test element is instrumented at each end, at the centre and at each end plate segment with thermocouples. The thermocouple tips are fastened to clean areas of the test element with Zircaloy shim material spot welded over them.

All instrument calibrations and checks were performed in accordance with written procedures. The thermocouples have an uncertainty of ±0.375% of reading and their calibration was checked with boiling water as the reference temperature. The linear potentiometer was calibrated (0 to 40 mm) against laboratory reference length standards and was found to have an uncertainty in the displacement measurement of ±0.1 mm. The load cell was calibrated (0 to 22.2 kN) and found to have an uncertainty in the load measurement of ±21 N. An alternate load cell (0 to 8.0 kN, F.S.) was used for Test #28 and those following because of the reduced loads being applied to the elements at this time.

CRACKED FUEL PELLET PREPARATION

Some of the tests required that the fuel pellets be cracked in order to simulate irradiated fuel. A mechanical press and die set was manufactured, shown in Figure 2 and a procedure developed to prepare the cracked fuel. Typical longitudinal and transverse cross sections of the mechanically cracked fuel are shown in Figures 3 and 4.

The element was inserted with the bearing pad up into the cracking rig and pressed between the dies. The pressing pressure was slowly increased to 4000 psi and decreased with a manually operated valve. This process was repeated four times with the element rotated to -90°, -45°, +45° and 180°, in that order with respect to the bearing pad. At 180°, the insert in the lower die was removed to allow the passage of the bearing pad and hence greater coverage of the element.

TEST PROCEDURE

A series of constant rate axial compression tests were performed at temperatures ranging from 300 to 1000 °C. The majority of the axial compression tests were performed at a constant compression rate of 3.0 $mm.s^{-1}$, but tests were also performed at compression rates of 2.0 $mm.s^{-1}$ and 0.25 $mm.s^{-1}$.

The overall length of each element before and after the test was measured. Throughout the tests, different measurements were taken as required such as the fuel pellet axial clearance, the element bow at the quarter and mid points and end cap projection height for example.

AXIAL COMPRESSION TESTS

The test housing was sealed, mounted into the compression rig and pressurized with Argon (<170 kPa) to ensure there were no major leaks. After a leak free system was established, the test housing interior was purged with Argon for about 10 minutes to eliminate any remaining air.

Power was applied to the ceramic heaters and the temperature was allowed to stabilize at the test temperature. With exception of the endcaps, the temperature gradient along the test element was typically less than ±10°C. The test housing was then isolated by closing the Argon purge gas valves to prevent loose UO_2 from escaping the rig.

The linear potentiometer was then zeroed, with the crosshead held manually against the element and the travel limit was set. The time dependent data acquisition was initiated then the axial load was applied to deform the element at a constant rate. The load was then removed, either automatically if the loading head displacement limit was reached, or manually if the maximum load was reached. The unloading curve was also measured.

The specimen was allowed to cool and filtered gas samples were checked for active material. Since no contamination was found, all post test measurements were done at Stern Laboratories. After the first compression test at 800°C and 25 mm of travel, the element was jammed into the test housing due to excessive distortion of the element. From this test on, the maximum load set point was reduced from 10 kN to approximately 4 kN and the maximum travel was reduced from 25 mm to less than 5 mm.

AXIAL COMPRESSION TESTS RESULTS

Tests 1 through 5 were conducted at various temperatures from 300°C to 800°C, with as-received fuel pellets and the spigots and end plate segments intact. The maximum load and travel were set at 10 kN and 25 mm for these tests. All these tests showed sheath ridging and buckling and the spigots had collapsed such that the end plate was in contact with the endcap. The severity of the distortions increased with the test temperature. Test 5, which was performed at 800°C, was jammed into the test section. After this test, the maximum load and travel were reduced to lessen the severity of the element distortions. Tests 6 and 7 were performed with the end plate segments and spigots removed and at 800°C. Figure 5 contains the load versus axial compression plots for these tests. The legend lists the test temperature with the test number in brackets. An overall element stiffness was extracted from these plots. The calculated stiffness is equal to the total change in load divided by the total axial compression. Plots of the calculated stiffness are shown in Figure 6.

Tests (8, 9, 10, 22, 23, 24, 25 and 28) were performed with the end plate segments and spigots removed, with as-received fuel pellets, at average temperatures from 300°C to 1100°C and the bearing pads facing up. The maximum load and travel were maintained below 5 kN and 5 mm, respectively. Figure 7 contains the load versus axial compression plots and Figure 8 contains the calculated stiffness plots for these tests.

Tests (14, 15, 16, 18, 19, 20, 21, 27 and 29) were performed with the end plate segments and spigots removed, with cracked fuel pellets, at average temperatures from 300°C to 1100°C and the bearing pads facing up. The maximum load and travel were maintained below 5 kN and 5.1 mm, respectively. Figure 9 contains the load versus axial compression plots and Figure 10 contains the calculated stiffness plots for these tests. These plots reveal that the stiffness is reasonably constant over the range of compressions tested and decreases with increasing average temperature. The peak stiffness of 1.4 $kN.mm^{-1}$ was at 300°C and the minimum was 0.3 $kN.mm^{-1}$ at 1100°C before decreasing with increasing compression. Tests (11, 12 and 13) were similarly configured and performed at 800°C to 1000°C but with a preliminary fuel pellet cracking procedure that resulted in fuel with a coarse structure.

The maximum axial compression for Test 29 was limited to approximately 2 mm. Total indicator readings (TIR) made on this element reveal that the maximum lateral deflection from the centreline of the element is 0.89 mm at 90° from the bearing pad centreline.

Tests (32, 33 and 34) were performed with the end plate segments and spigots intact, with cracked fuel pellets, at an average temperature of 900°C, the bearing pads facing down and at various axial compression rates. The compression rate was 2 $mm.s^{-1}$ for Test 32 and 0.25 $mm.s^{-1}$ for Tests 33 and 34. Test 33 is suspect since for a given compression the load was low, ie. low stiffness. Post test observations showed that the element was improperly seated into the loading head. Both Tests 33 and 34 were loaded more than once to increasing compression limits. Figure 11 contains the load versus axial compression plots for Tests 29, 32 and 34. These plots show insignificant effects on the stiffness due to the compression rate over the range tested.

DISCUSSION AND CONCLUSIONS

The test results indicate that there was significant accommodation of the fuel in axial compression. The degree of accommodation is dependent upon the temperature, and the mechanical state of the UO_2 fuel pellets (i.e., cracked or intact).

1. The highest load was measured in compressing the uncracked fuel element. This load exceeded 10 kN for an axial compression of 10 to 21.5 mm. The end spigots also deformed during these tests. The greatest deformation occurred at the highest temperature (800 °C).

2. The highest load measured in compressing the uncracked fuel element without end plate spigots was 4.8 kN with an axial compression of 3 to 5 mm. The load did not appear to be very sensitive to the temperature of testing.

3. The highest load recorded in compressing the cracked fuel elements was 4.5 kN at 500 °C and with no spigots on the endcaps. The loads did decrease with temperature, dropping to about 1.5 kN for an axial compression of 4 to 5 mm.

4. The compression rate did not have a large effect on the load curves at 900 °C.

5. For axial compressions of less than 2 mm (between the endcaps, no spigots) the fuel sheath was found not to contact neighbouring surfaces.

The results supported Ontario Hydro's safety analysis and demonstrated a significant conservatism in the modelling of the axial loading under conditions of constrained axial expansion. The forces required to compress a fuel element axially, in order to accommodate predicted excess axial expansions at elevated fuel temperatures, are significantly less than the analysis prediction.

REFERENCES:

1 G.J. Field, "Bruce and Darlington Power Pulse and Pressure Tube Integrity Program", Proceedings of the 15th Annual CNS conference, Montreal Quebec, ISSS 0227-1907, June 1994.

2 J.K. Chan, Y. Liu, H.E. Sills, and V.J. Langman, "High Temperature Fuel Behaviour, Constrained Axial Expansion and the Potential Effects on Fuel Channel Integrity During Large Break LOCAs", Ontario Hydro RSOAD Report no. N-03503.7-955045, April 4, 1995.

3 B.A.W. Smith, B.H. Rod, "Out-Reactor Axial Stiffness Measurements of Irradiated Darlington Fuel elements", AECL-CRL report RC-897, March 1993.

4 R.E. Williford, "A Cracked-Fuel Constitutive Equation", Nuclear Technology, vol 67, p208, 1984.

5 I.J. Hastings, "Structures in Irradiated UO_2 Fuel from Canadian Reactors", Atomic Energy of Canada Ltd. Report AECL-MISC-249, October 1982.

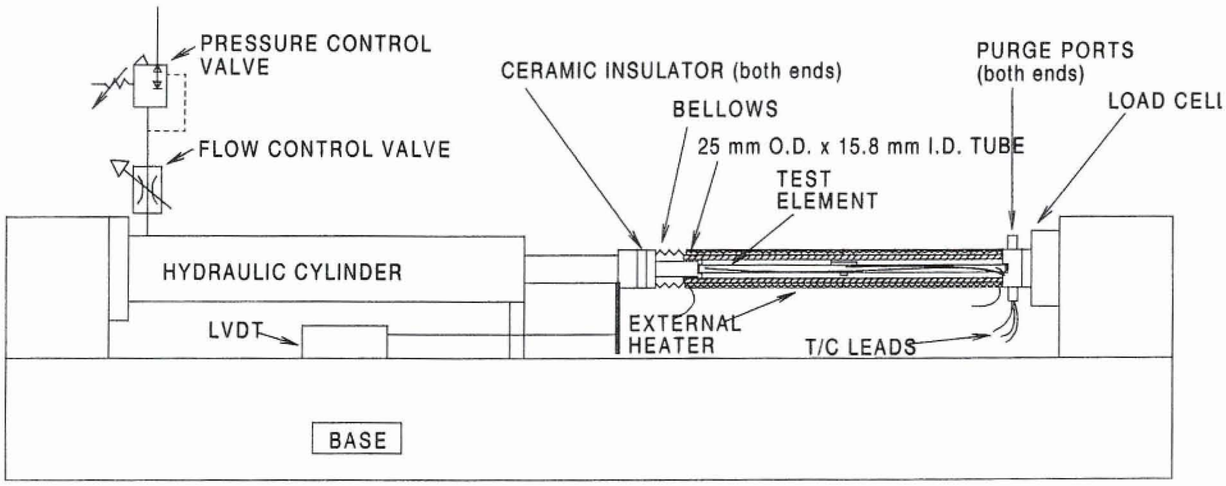

FIGURE 1: SINGLE ELEMENT TEST ASSEMBLY

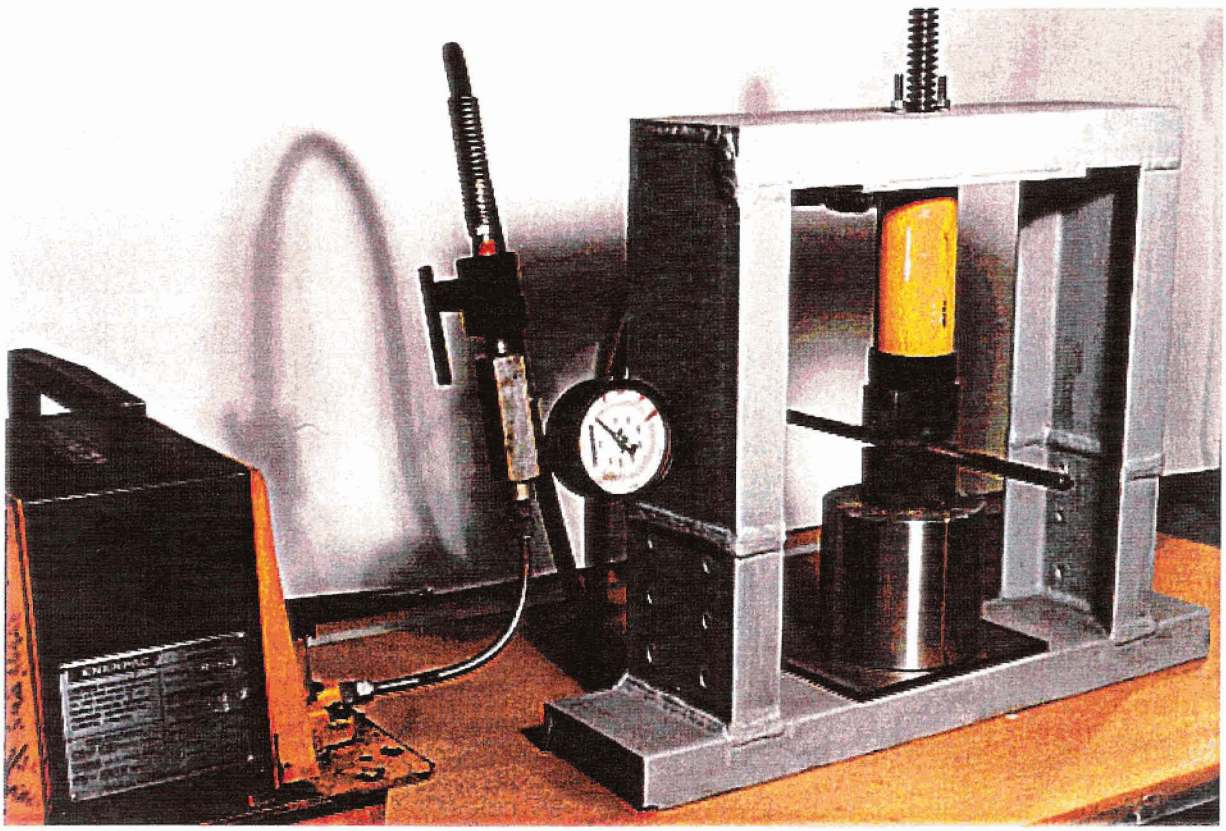

FIGURE 2: FUEL PELLET CRACKING RIG

FIGURE 3: LONGITUDINAL CROSS SECTION

FIGURE 4: TRANSVERSE CROSS SECTION

Uncraked As-Received Element

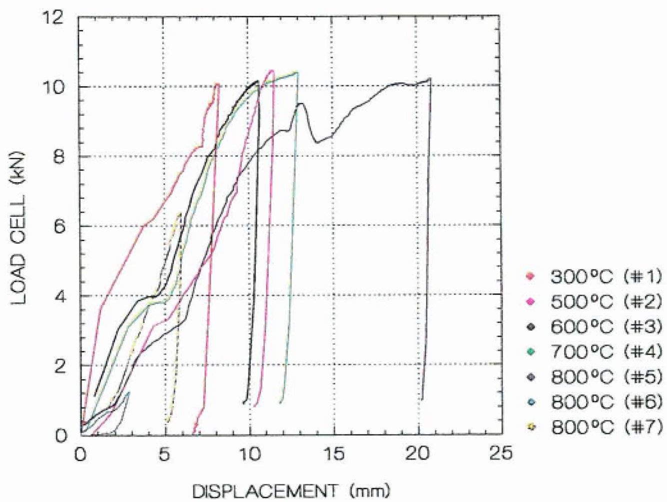

Figure 5: Load vs. Axial Compression

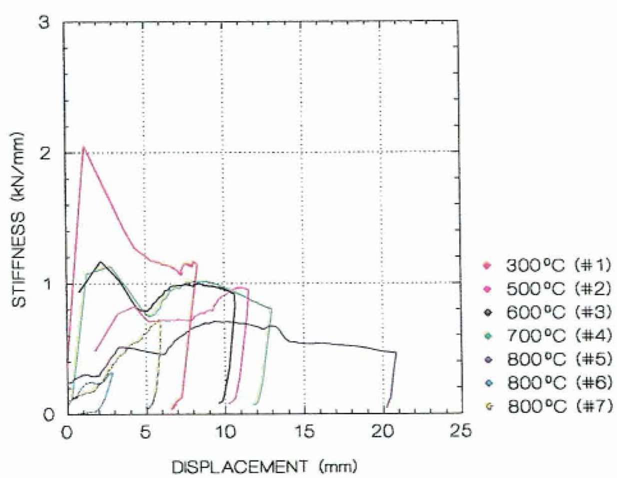

Figure 6: Element Stiffness vs. Axial Compression

Uncracked As-Received Element (Endplate, Spigot Removed)

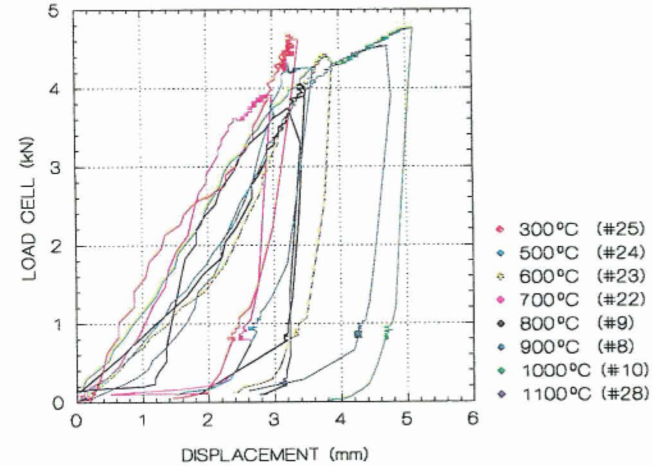

Figure 7: Load vs. Axial Compression

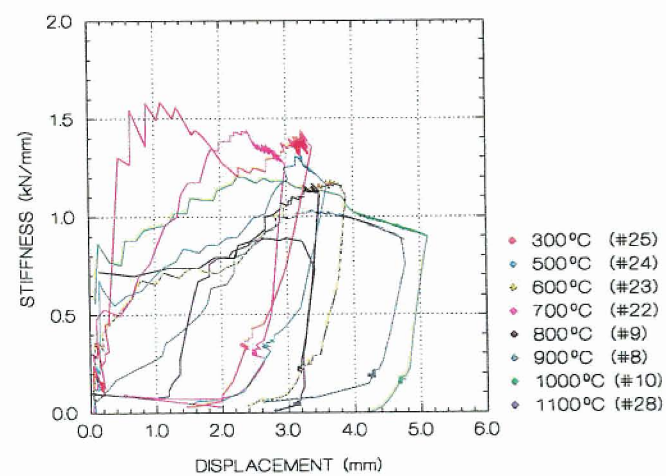

Figure 8: Element Stiffness vs. Axial Compression

Crakced As-Received Element (Endplate and Spigot Removed)

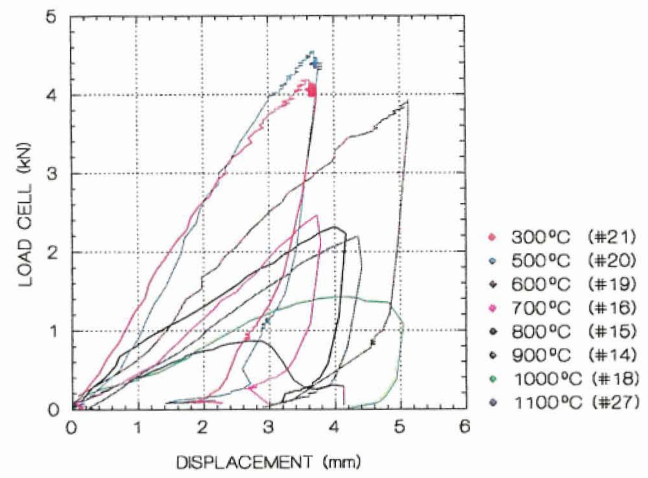

Figure 9: Load vs. Axial Compression

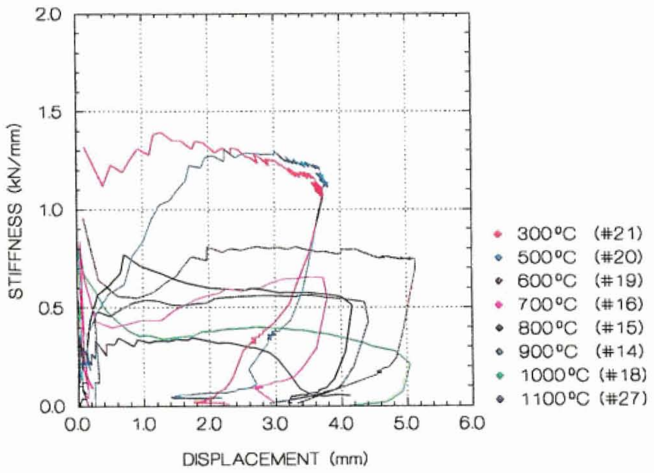

Figure 10: Element Stiffness vs. Axial Compression

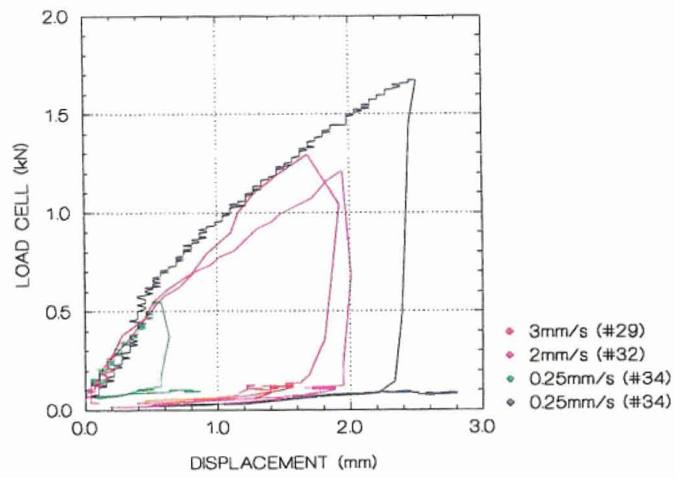

Figure 11: Effect of Axial Compression Rate on Axial Loading